



US009608198B2

(12) **United States Patent**  
**Yuasa**

(10) **Patent No.:** **US 9,608,198 B2**  
(45) **Date of Patent:** **\*Mar. 28, 2017**

(54) **MAGNETIC TUNNEL JUNCTION DEVICE**

(71) Applicants: **Japan Science and Technology Agency**, Kawaguchi-shi, Saitama (JP); **National Institute of Advanced Industrial Science and Technology**, Tokyo (JP)

(72) Inventor: **Shinji Yuasa**, Ibaraki (JP)

(73) Assignees: **JAPAN SCIENCE AND TECHNOLOGY AGENCY**, Saitama (JP); **NATIONAL INSTITUTE OF ADVANCED INDUSTRIAL SCIENCE AND TECHNOLOGY**, Tokyo (JP)

(\* ) Notice: Subject to any disclaimer, the term of this patent is extended or adjusted under 35 U.S.C. 154(b) by 0 days.

This patent is subject to a terminal disclaimer.

(21) Appl. No.: **14/837,558**

(22) Filed: **Aug. 27, 2015**

(65) **Prior Publication Data**

US 2016/0020385 A1 Jan. 21, 2016

**Related U.S. Application Data**

(63) Continuation of application No. 13/767,290, filed on Feb. 14, 2013, now Pat. No. 9,123,463, which is a (Continued)

(30) **Foreign Application Priority Data**

Mar. 12, 2004 (JP) ..... 2004-071186  
Oct. 28, 2004 (JP) ..... 2004-313350

(51) **Int. Cl.**

**H01L 43/10** (2006.01)  
**H01F 10/13** (2006.01)

(Continued)

(52) **U.S. Cl.**

CPC ..... **H01L 43/10** (2013.01); **B82Y 25/00** (2013.01); **G11C 11/15** (2013.01); **G11C 11/16** (2013.01);

(Continued)

(58) **Field of Classification Search**

CPC ..... G11C 11/161; G11C 11/15; G11C 11/16; H01F 10/132; H01F 10/3254; H01L 28/55;

(Continued)

(56) **References Cited**

**U.S. PATENT DOCUMENTS**

5,239,504 A 8/1993 Brady et al.  
5,506,063 A 4/1996 Kamijo et al.

(Continued)

**FOREIGN PATENT DOCUMENTS**

EP 0 145 403 6/1985  
EP 1 061 592 12/2000

(Continued)

**OTHER PUBLICATIONS**

International Search Report of PCT/JP2005/004720 mailed Jun. 21, 2005.

(Continued)

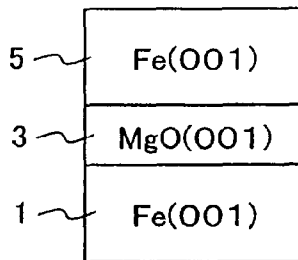
*Primary Examiner* — Alonzo Chambliss

(74) *Attorney, Agent, or Firm* — Nicholas Trenkle; Stites & Harbison, PLLC.

(57) **ABSTRACT**

The output voltage of an MRAM is increased by means of an Fe(001)/MgO(001)/Fe(001) MTJ device, which is formed by microfabrication of a sample prepared as follows: A single-crystalline MgO (001) substrate is prepared. An epitaxial Fe(001) lower electrode (a first electrode) is grown on a MgO(001) seed layer at room temperature, followed by annealing under ultrahigh vacuum. A MgO(001) barrier layer is epitaxially formed on the Fe(001) lower electrode

(Continued)



(the first electrode) at room temperature, using a MgO electron-beam evaporation. A Fe(001) upper electrode (a second electrode) is then formed on the MgO(001) barrier layer at room temperature. This is successively followed by the deposition of a Co layer on the Fe(001) upper electrode (the second electrode). The Co layer is provided so as to increase the coercive force of the upper electrode in order to realize an antiparallel magnetization alignment.

6 Claims, 10 Drawing Sheets

Related U.S. Application Data

continuation of application No. 13/400,340, filed on Feb. 20, 2012, now Pat. No. 8,405,134, which is a continuation of application No. 12/923,643, filed on Sep. 30, 2010, now Pat. No. 8,319,263, which is a continuation of application No. 10/591,947, filed as application No. PCT/JP2005/004720 on Mar. 10, 2005, now Pat. No. 7,884,403.

(51) Int. Cl.

- G11C 11/15* (2006.01)
- H01L 49/02* (2006.01)
- H01L 27/11507* (2017.01)
- B82Y 25/00* (2011.01)
- G11C 11/16* (2006.01)
- H01F 10/32* (2006.01)
- H01L 43/08* (2006.01)
- H01L 43/12* (2006.01)
- H01L 43/02* (2006.01)
- H01L 27/22* (2006.01)
- B82Y 10/00* (2011.01)

(52) U.S. Cl.

- CPC ..... *H01F 10/132* (2013.01); *H01F 10/3254* (2013.01); *H01L 27/11507* (2013.01); *H01L 27/228* (2013.01); *H01L 28/55* (2013.01); *H01L 43/02* (2013.01); *H01L 43/08* (2013.01); *H01L 43/12* (2013.01); *B82Y 10/00* (2013.01); *H01L 27/22* (2013.01)

(58) Field of Classification Search

- CPC . H01L 27/11507; H01L 27/22; H01L 27/228; H01L 43/08; H01L 43/10; H01L 43/12; B82Y 10/00; B82Y 25/00

See application file for complete search history.

6,911,685 B2	6/2005	Anthony et al.	
6,927,952 B2	8/2005	Shimizu et al.	
6,999,287 B2	2/2006	Hayashi et al.	
7,149,105 B2	12/2006	Brown	
7,220,498 B2	5/2007	Nagahama et al.	
7,252,852 B1	8/2007	Parkin	
7,262,064 B2	8/2007	Ohba et al.	
7,270,896 B2	9/2007	Parkin	
7,276,384 B2	10/2007	Parkin et al.	
7,408,749 B2	8/2008	Gill	
7,443,639 B2	10/2008	Parkin	
7,453,672 B2	11/2008	Dieny et al.	
7,570,463 B2	8/2009	Parkin	
7,598,555 B1	10/2009	Papworth Parkin	
7,884,403 B2	2/2011	Yuasa	
8,319,263 B2 *	11/2012	Yuasa	B82Y 25/00
			257/295
8,405,134 B2 *	3/2013	Yuasa	B82Y 25/00
			257/295
9,123,463 B2 *	9/2015	Yuasa	B82Y 25/00
2002/0064595 A1	5/2002	Nomura et al.	
2002/0080641 A1	6/2002	Asao et al.	
2002/0149962 A1	10/2002	Horiguchi	
2002/0159203 A1	10/2002	Saito et al.	
2002/0191355 A1	12/2002	Hiramoto et al.	
2003/0128483 A1	7/2003	Kamijo	
2003/0203189 A1	10/2003	Futamoto et al.	
2004/0001372 A1	1/2004	Higo et al.	
2004/0082201 A1	4/2004	Sharma et al.	
2004/0136232 A1	7/2004	Hosomi et al.	
2004/0139914 A1	7/2004	Yamazaki et al.	
2004/0144995 A1	7/2004	Nagahama et al.	
2004/0234818 A1	11/2004	Tanahashi et al.	
2004/0245553 A1	12/2004	Hosomi et al.	
2004/0257719 A1	12/2004	Ohba et al.	
2005/0047027 A1	3/2005	Lin et al.	
2005/0110004 A1	5/2005	Parkin et al.	
2005/0207071 A1	9/2005	Sato et al.	
2006/0003185 A1	1/2006	Parkin	
2006/0012926 A1	1/2006	Parkin	
2006/0049441 A1	3/2006	Janesky et al.	
2006/0056115 A1	3/2006	Djayaprawira et al.	
2006/0125034 A1	6/2006	Ohba et al.	
2006/0261425 A1	11/2006	Suemitsu et al.	
2007/0128470 A1	6/2007	Nagahama et al.	
2007/0195592 A1	8/2007	Yuasa	
2007/0258170 A1	11/2007	Yuasa	
2008/0055793 A1	3/2008	Djayaprawira et al.	
2008/0062581 A1	3/2008	Parkin	
2008/0124454 A1	5/2008	Djayaprawira et al.	
2008/0180862 A1	7/2008	Djayaprawira et al.	
2008/0182342 A1	7/2008	Parkin	
2008/0212243 A1	9/2008	Zhao et al.	
2008/0253039 A1	10/2008	Nagamine et al.	
2009/0128167 A1	5/2009	Hamada et al.	
2009/0324814 A1	12/2009	Parkin	

FOREIGN PATENT DOCUMENTS

(56)

References Cited

U.S. PATENT DOCUMENTS

5,514,484 A	5/1996	Nashimoto
5,759,265 A	6/1998	Nashimoto et al.
5,800,635 A	9/1998	Collins et al.
5,817,366 A	10/1998	Arai et al.
5,945,694 A	8/1999	Reyes et al.
6,054,226 A	4/2000	Takeda et al.
6,181,537 B1	1/2001	Gill
6,201,672 B1	3/2001	Pinarbasi
6,252,750 B1	6/2001	Gill
6,275,362 B1	8/2001	Pinarbasi
6,379,978 B2	4/2002	Goebel et al.
6,544,801 B1	4/2003	Slaughter et al.
6,767,655 B2	7/2004	Hiramoto et al.
6,819,586 B1	11/2004	Anthony et al.
6,828,260 B2	12/2004	Sharma et al.
6,831,312 B2	12/2004	Slaughter et al.
6,839,206 B2	1/2005	Saito et al.

EP	1 085 586	3/2001
EP	1 391 942	5/2002
EP	1 494 295	1/2005
EP	1 633 007	3/2006
EP	1 793 434	6/2007
JP	H05-144729	6/1993
JP	11-097766	4/1999
JP	2000-030236	1/2000
JP	2001-101645	4/2001
JP	2002-20400	7/2002
JP	2002-204004	7/2002
JP	2002-246567	8/2002
JP	2002-270790	9/2002
JP	2002-270921	9/2002
JP	2002-289943	10/2002
JP	2002-319722	10/2002
JP	2002-359413	12/2002
JP	2003-86863	3/2003
JP	2003-283001	10/2003
JP	2003-304010	10/2003

(56)

## References Cited

## FOREIGN PATENT DOCUMENTS

JP	2003-304012	10/2003
JP	2003-318465	11/2003
JP	2004-022599	1/2004
JP	2004-022599	1/2004
JP	2004-063592	2/2004
JP	2004-128015	4/2004
JP	2004-153258	5/2004
JP	2006-080116	3/2006
JP	2008-004956	1/2008
KR	2002-0042448	6/2002
KR	2003-0097904	12/2003
WO	WO 01/56090	8/2001
WO	WO 02/99905	5/2002
WO	WO 03/085750	10/2003
WO	WO 2004/025744	3/2004
WO	WO 2005/088745	9/2005

## OTHER PUBLICATIONS

- Wolf, S.A. et al., "Spintronics: A Spin-Based Electronics Vision for the Future", *Science*, vol. 294, Nov. 16, 2001, pp. 1488-1495.
- Wulfhekel, W. et al., "Single-Crystal Magnetotunnel Junctions", *Applied Physics Letters*, vol. 78, No. 4, Jan. 22, 2001, pp. 509-511.
- Julliere, M., "Tunneling Between Ferromagnetic Films", *Physics Letters*, vol. 54A, No. 3, Sep. 8, 1975, pp. 225-226.
- Soulen, R.J., Jr. et al., "Measuring the Spin Polarization of a Metal with a Superconducting Point Contact", *Science*, vol. 282, Oct. 2, 1998, pp. 85-88.
- Saito, Y. et al., "Correlation between Barrier Width, Barrier Height, and DC Bias Voltage Dependences on the Magnetoresistance Ratio in Ir-Mn Exchange Biased Single and Double Tunnel Junctions", *Jpn. J. Appl. Phys.*, vol. 39 (2000), pp. L1035-L1-38.
- Iura, S. et al., "Enhancement of Thermal Stability in Ferromagnetic Tunnel Junctions Prepared by the Radical Oxidation Method", *Journal of the Magnetics Society of Japan*, vol. 26, No. 6 (2002), pp. 839-842, abstract only in English.
- Bowen, M. et al., "Large Magnetoresistance in Fe/MgO/FeCo(001) Epitaxial Tunnel Junctions on GaAs(001)", *Applied Physics Letters*, vol. 79, No. 11, Sep. 10, 2001, pp. 1655-1657.
- Simmons, John G., "Generalized Formula for the Electric Tunnel Effect between Similar Electrodes Separated by a Thin Insulating Film", *Journal of Applied Physics*, vol. 34, No. 6, Jun. 1963, pp. 1793-1803.
- Vassent, J.L. et al., "A Study of Growth and the Relaxation of Elastic Strain in MgO on Fe(001)", *J. Appl. Phys.* vol. 80, No. 10, Nov. 15, 1996, pp. 5727-5735.
- Faure-Vincent, J. et al., "High Tunnel Magnetoresistance in Epitaxial Fe/MgO/Fe Tunnel Junctions", *Applied Physics Letters*, vol. 82, No. 25, Jun. 23, 2003, pp. 4507-4509. X.
- Meyerheim, H.L. et al., "Geometrical and Compositional Structure at Metal-Oxide Interfaces: MgO on Fe(001)", *Physical Review Letters*, vol. 18, No. 7, Aug. 13, 2001, pp. 076102-1-076102-4.
- Butler, W.H. et al., "Spin-dependent Tunneling Conductance of Fe[MgO]Fe Sandwiches", *Physical Review B*, vol. 63, 054416, 2001, pp. 054416-1-054416-12.
- Mathon, J. et al., "Theory of Tunneling Magnetoresistance of an Epitaxial Fe/MgO/Fe(001) Junction", *Physical Review B*, vol. 63, 220403(R), 2001, pp. 220403-1-220403-4.
- Zhang, X.-G. et al., "Effects of the Iron-Oxide Layer in Fe—FeO—MgO—Fe Tunneling Junctions", *Physical Review B*, vol. 68, 092402, 2003, pp. 092402-1-092402-4.
- Zhang, X.-G. et al., "Large Magnetoresistance in bcc Co/MgO/Co and FeCo/MgO/FeCo Tunnel Junctions", *Physical Review B*, vol. 70, 172407, 2004, pp. 172407-1-172407-4.
- Gibson, A. et al., "Stability of Vacancy Defects in MgO: The Role of Charge Neutrality", *Physical Review B*, vol. 50, No. 4, Jul. 15, 1994—II, pp. 2582-2592.
- Yuasa, S. et al., "High Tunnel Magnetoresistance at Room Temperature in Fully Epitaxial Fe/MgO/Fe Tunnel Junctions Due to Coherent Spin-Polarized Tunneling", *Japanese Journal of Applied Physics*, vol. 43, No. 4B, 2004, pp. L588-L590.
- Mitani, S., et al., "Fe/MgO/FeCo (100) Epitaxial Magnetic Tunnel Junctions Prepared by Using in situ Plasma Oxidation", *Journal of Applied Physics*, vol. 93, No. 10, Parts 2 and 3, May 15, 2003, pp. 8041-8043.
- Popova, E., et al., "Epitaxial MgO Layer for Low-Resistance and Coupling-Free Magnetic Tunnel Junctions", *Applied Physics Letters*, vol. 81, No. 6, Aug. 5, 2002, pp. 1035-1037.
- Boubeta, C. Martinez, et al., "Magnetic Coupling in Epitaxial TM/MgO/Fe(001) (TM=FeCo, Fe/Co, Fe) Macroscopic and Microscopic Trilayers", *Journal of Applied Physics*, Vol. 94, No. 6, Sep. 15, 2003, pp. 4006-4012.
- Supplementary European Search Report from European Patent Office for Application No. 05720955.3 2222, Patent No. 1737055, PCT/JP2005004720 dated Jul. 2, 2008.
- Office Action from European Patent Office dated Nov. 6, 2009.
- F. Ernult et al., "Preparation of Nanometer-Scale Iron Dots on Insulating Layer", *Science and Technology of Advanced Materials*, vol. 4, (2003), pp. 383-389.
- David J. Smith et al., "Structural Characterization of Thin Film Ferromagnetic Tunnel Junctions", *Journal of Applied Physics*, vol. 83, No. 10, May 15, 1998, pp. 5154-5158.
- X. W. Li et al., "Fabrication and Properties of Heteroepitaxial Magnetite (Fe<sub>3</sub>O<sub>4</sub>) Tunnel Junctions", *Applied Physics Letters*, vol. 73, No. 22, Nov. 30, 1998, pp. 3282-3284.
- C. L. Platt, et al., "Spin Polarized Tunneling in Reactively Sputtered Tunnel Junctions", *Journal of Applied Physics*, vol. 81, No. 8, Apr. 15, 1997, pp. 5523-5525.
- P. Turban et al., "Growth and Characterization of Single Crystalline NiMnSb Thin Films and Epitaxial NiMnSb/MgO/NiMnSb(001) Trilayers", 2002 The American Physical Society, *Physical Review B*, vol. 65, pp. 134417-1 to 134417-13.
- T. Moriyama et al., "Preparation and Magnetoresistance in Single-Crystal and Polycrystal Fe/MgO/FeCo Tunnel Junctions", *The Physical Society of Japan, 2003 Spring meeting, Abstracts Book 58(1-3)*, 460, (Mar. 6, 2003).
- Jagadeesh S. Moodera et al., Ferromagnetic-Insulator-Ferromagnetic Tunneling: Spin-Dependent Tunneling and Large Magnetoresistance in Trilayer Junctions (Invited), *Journal of Applied Physics*, vol. 79, No. 8, Apr. 15, 1996, pp. 4724-4729.
- Masayoshi Tonouchi et al., "Epitaxial Growth of NbN on an Ultrathin MgO/Semiconductor System", *Journal of Applied Physics*, vol. 62, No. 3, Aug. 1, 1987, pp. 961-966.
- "Giant tunnel magnetoresistance in magnetic tunnel junctions with a crystalline MgO(001) barrier," S. Yuasa and D.D. Djayapawira, *Journal of Applied Physics D: Applied Physics*, 1 Phys. D: Appl. Phys. 40 (2007) R337-R354.
- Office Action issued from Japanese Patent Office, in corresponding Japanese Patent Application No. 2011-226907, dated Jan. 31, 2012, pp. 1-3.
- Araki et al., "Fabrication and Electric Properties of Lapped Type of TMR Heads for ~50 Gb/In<sup>2</sup> and Beyond," *IEEE Transactions on Magnetics*, vol. 38, No. 1, pp. 72-77, Jan. 2002.
- David D. Djayapawira et al., "230% Room-Temperature Magnetoresistance in CoFeB/MgO/CoFeB, Magnetic Tunnel Junctions," *IEICE Technical Report*, vol. 104, No. 713, Mar. 4, 2005.
- David D. Djayapawira et al., "Novel Sputtering Technology of Magnetic Tunnel Junctions for MRAM Application," *Papers of the 66<sup>th</sup> Symposium on Semiconductors and Integrated Circuits Technology*, vol. 66, pp. 58-61, 2004.
- H. Domon et al., "Effect of Ge Addition on Postannealed CoCrGePt Thin Film Media," *Journal of Applied Physics*, vol. 91, No. 10, pp. 8632-8634, May 15, 2002.
- H. Domon et al., "Reduction of Magnetic Interaction in CoB/Pd Multilayer Perpendicular Media Using a Phase-Separated Pd-SiO Underlayer," *Journal of Applied Physics*, vol. 93, No. 10, pp. 8164-8166, May 15, 2003.
- Extended European Search Report, issued from European Patent Office, of European Application No. 08159511.8, dated Jun. 5, 2009.

(56)

## References Cited

## OTHER PUBLICATIONS

- T. Kakuta et al., "Novel PVD Tool for Magnetoresistive Random Access Memory (MRAM) Mass Production," Anelva Technical Report, vol. 10, pp. 27-33, Jan. 25, 2004.
- A. Kobayashi et al., "TMR Devices Fabricated with RIE Etching Using  $\text{Co} + \text{NH}_3$ ," Journal of the Magnetism Society of Japan, vol. 28, No. 2, Feb. 1, 2004.
- J.S. Moodera et al., "Large Magnetoresistance at Room Temperature in Ferromagnetic Thin Film Tunnel Junctions," Physical Review Letters, vol. 74, No. 16, pp. 3273-3276, Apr. 17, 1995.
- J.S. Moodera, "Interface Magnetism and Spin Wave Scattering in Ferromagnet-Insulator-Ferromagnet Tunnel Junctions," Physical Review Letters, vol. 80, No. 13, pp. 2941-2944, Mar. 30, 1998.
- J. Murai et al., "Direct Observation of Magnon Excitation in a Ferromagnetic Tunnel Junction Using Inelastic-Electron-Tunneling Spectroscopy," Japanese Journal of Applied Physics, vol. 38, pp. L1106-L1108, Oct. 1, 1999.
- K. Nagasaka et al., "CPP Operational Mode of GMR Head," Fujitsu Sci. Tech. J., vol. 37, No. 2, pp. 192-200, Dec. 2001.
- T. Osada et al., "Dry Etching of Magnetic Thin Film Stacks Using  $\text{CO}/\text{NH}_3$  and  $\text{CH}_3\text{OH}$  Gases for Tunneling Magneto-Resistance Devices," 2004 Dry Process International Symposium, vol. 4, pp. 127-131, 2004.
- Stuart S.P. Parkin et al., "Giant Tunneling Magnetoresistance at Room Temperature with  $\text{MgO}$  (100) Tunnel Barriers," Nature Materials, vol. 3, pp. 862-867, Dec. 2004.
- M. Takagishi et al., "The Applicability of CPP-GMR Heads for Magnetic Recording," IEEE Transactions on Magnetics, vol. 38, No. 5, pp. 2277-2282, Sep. 2002.
- A. Tanaka et al., "Spin-Valve Heads in the Current-Perpendicular-to-Plane Mode for Ultrahigh-Density Recording," IEEE Transactions on Magnetics, vol. 38, No. 1, Jan. 2002.
- K. Tsunekawa et al., "Surface Treatment Techniques in Fabrication of GMR and TMR Films," Journal of the Magnetism Society of Japan, vol. 28, No. 11, pp. 1074-1080, Nov. 1, 2004.
- D. Wang et al., "70% TMR at Room Temperature for SDT Sandwich Junctions With  $\text{CoFeB}$  as Free and Reference Layers," IEEE Transactions on Magnetics, vol. 40, No. 4, pp. 2270-2271, Jul. 2004.
- S. Yoshimura et al., "Magnetic Grain Size Reduction by Using Oxygen Exposure Process Onto Very Thin Islandlike  $\text{WCr}$  Seedlayer in Longitudinal Recording Media," Journal of Applied Physics, vol. 91, No. 10, pp. 8629-8631, May 15, 2002.
- S. Yoshimura et al., "Grain Size Reduction by Utilizing a Very Thin, High-Melting-Point  $\text{WCr}$  Seedlayer in Longitudinal Media: Media Noise Reduction in High  $H_k^{\text{grain}}$  Media," vol. 25, No. 4-2, pp. 627-630 (2001).
- Yu et al., "Electron Transport Properties in Magnetic Tunnel Junctions with Epitaxial  $\text{NiFe}$  (111) Ferromagnetic Bottom Electrodes," Applied Physics Letters, vol. 82, No. 26, pp. 4735-4737, Jun. 30, 2003.
- S. Yuasa et al., "Magnetic Tunnel Junctions With Single-Crystal Electrodes: A Crystal Anisotropy of Tunnel Magneto-Resistance," Europhysics Letters, vol. 52, No. 3, pp. 344-350 Nov. 1, 2000.
- S. Yuasa et al., "Giant Room-Temperature Magnetoresistance in Single-Crystal  $\text{Fe}/\text{MgO}/\text{Fe}$  Magnetic Tunnel Junctions," Nature Materials vol. 3, pp. 868-871, Oct. 31, 2004.
- S. Yuasa et al., "Spin-Polarized Resonant Tunneling in Magnetic Tunnel Junctions," Science, vol. 297, pp. 234-237, Jul. 12, 2002.
- S. Zhang et al., "Quenching of Magnetoresistance by Hot Electrons in Magnetic Tunnel Junctions," Physical Review Letters, vol. 79, No. 19, pp. 3744-3747, Nov. 10, 1997.
- Shang, et al., "The First-principles Study of Electronic Structure of  $\text{Fe}/\text{MgO}/\text{Fe}$  Magnetic Tunnel Junctions Interface", 2005, pp. 2255-2258, vols. 475-479, Materials Science Forum.
- Meyerheim, et al., "Surface X-Ray Diffraction Analysis of the  $\text{MgO}/\text{Fe}(001)$  Interface: Evidence for an FEO Layer", 2002, pp. 144433-1-144433-7, vol. 65, Physical Review.
- Djayaprawira, et al., "230% Room-Temperature Magnetoresistance in  $\text{CoFeB}/\text{MgO}/\text{CoFeB}$  Magnetic Tunnel Junctions" 2005, pp. 092502-1-092502-3, vol. 86, Appl. Phys. Lett.
- Miyokawa, et al., "X-Ray Absorption and X-Ray Magnetic Circular Dichroism Studies of a Monatomic  $\text{Fe}(001)$  Layer Facing a Single-Crystalline", 2005, pp. L9-L11, vol. 44, No. 1, Japanese Journal of Applied Physics.
- Klaua, et al., "Growth, Structure, Electronic, and Magnetic Properties of  $\text{MgO}/\text{Fe}(001)$  Bilayers and  $\text{Fe}/\text{MgO}/\text{Fe}(001)$  Trilayers" 2001, vol. 64, pp. 134411-1-134411-8, Physical Review B.
- Mitani, et al., " $\text{Fe}/\text{MgO}/\text{FeCo}(100)$  Epitaxial Magnetic Tunnel Junctions Prepared by Using in situ Plasma Oxidation" May 15, 2003, pp. 8041-8043, vol. 93, No. 10, parts 2 & 3, J. Appl. Phys.
- Yuasa, et al., "Giant Room-Temperature Magnetoresistance in Single-Crystal  $\text{Fe}/\text{MgO}/\text{Fe}$  Magnetic Tunnel Junctions" Dec. 2004, pp. 868-871, vol. 3, Nature materials.
- Nozaki, et al., "Bias Voltage Effect on Tunnel Magnetoresistance in Fully Epitaxial  $\text{MgO}$  Double-Barrier Magnetic Tunnel Junctions" 2005, pp. 082501-1-082501-3, vol. 86, Appl. Phys. Lett.
- Butler, et al., "Spin-Dependent Tunneling and Conductance of  $\text{Fe}/\text{MgO}/\text{Fe}$  Sandwiches", 2001, pp. 054416-1-054416-11, vol. 63, Physical Review.
- Zhang, et al., "Large Magnetoresistance in BCC.  $\text{Co}/\text{MgO}/\text{Co}$  and  $\text{FeCo}/\text{MgO}/\text{FeCo}$  Tunneling Junctions", Nov. 17, 2012, pp. 1-9.
- Boubeta, et al., "Magnetization Reversal and Magnetic Anisotropies in Epitaxial  $\text{Fe}/\text{MgO}$  and  $\text{Fe}/\text{MgO}/\text{Fe}$  heterostructures grown on  $\text{Si}(001)$ ", Feb. 15, 2003, pp. 2126-2134, vol. 93, No. 4, J. Appl. Phys.

\* cited by examiner

FIG. 1 (A)

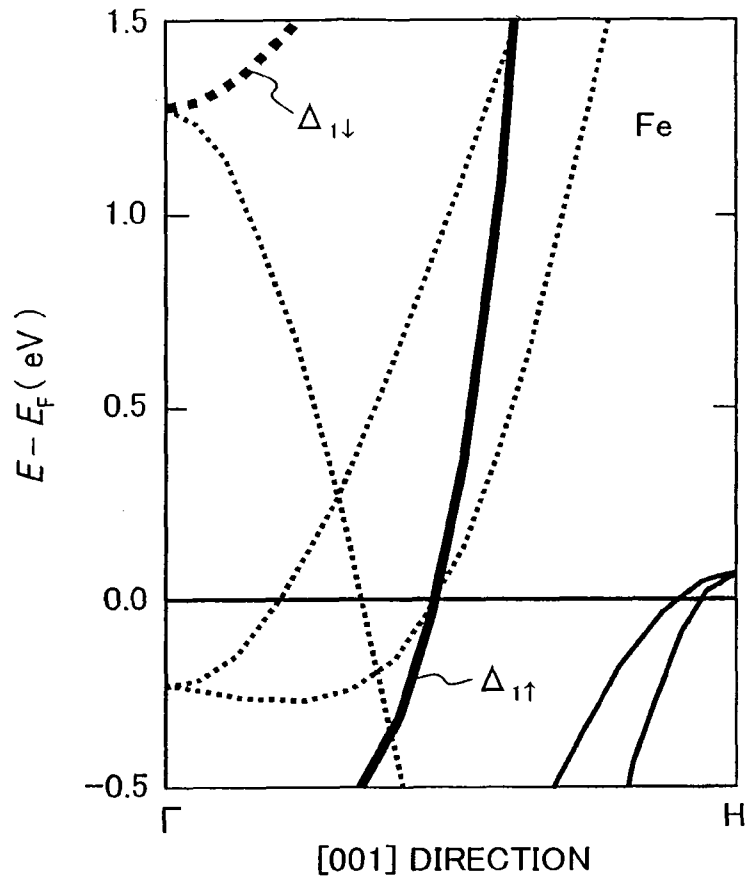


FIG. 1 (B)

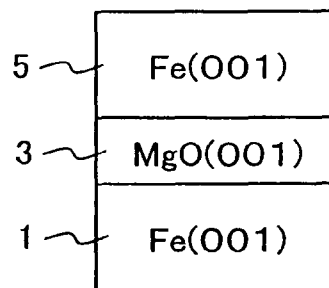


FIG. 2 (A)

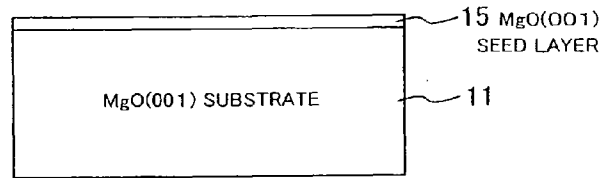


FIG. 2 (B)

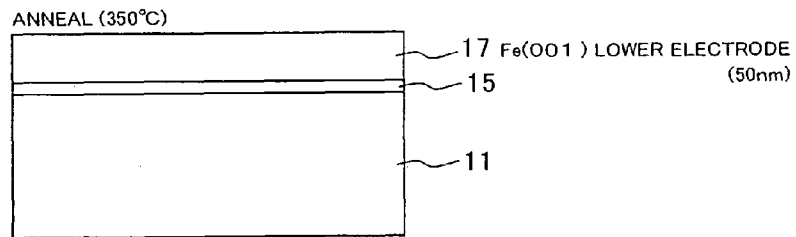


FIG. 2 (C)

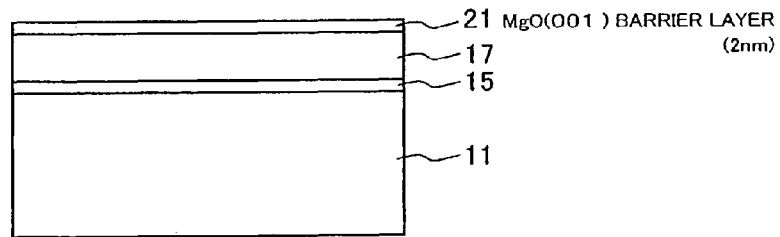


FIG. 2 (D)

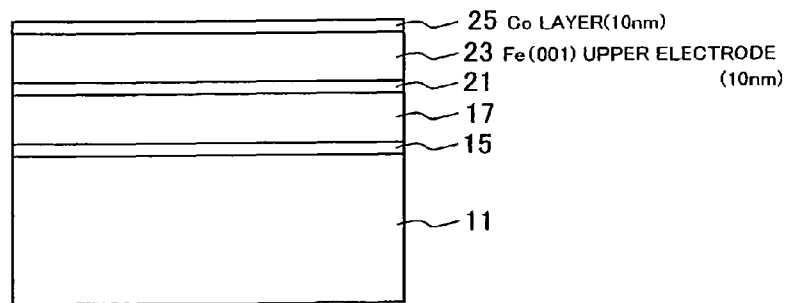


FIG. 3 (A)

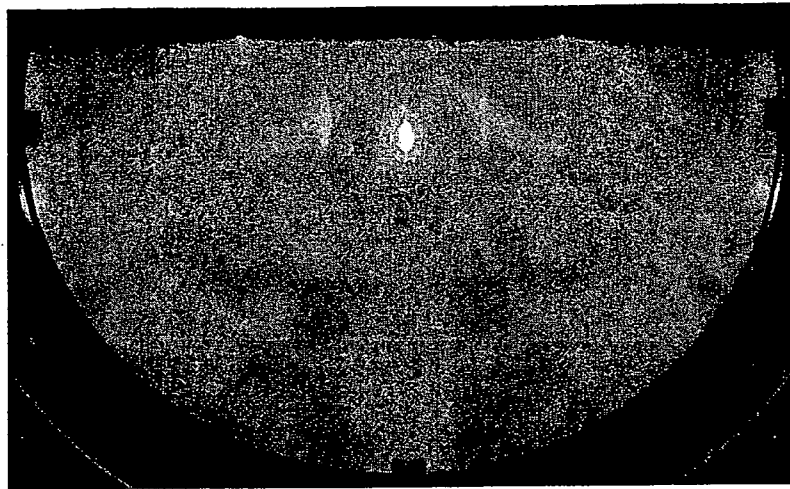


FIG. 3 (B)

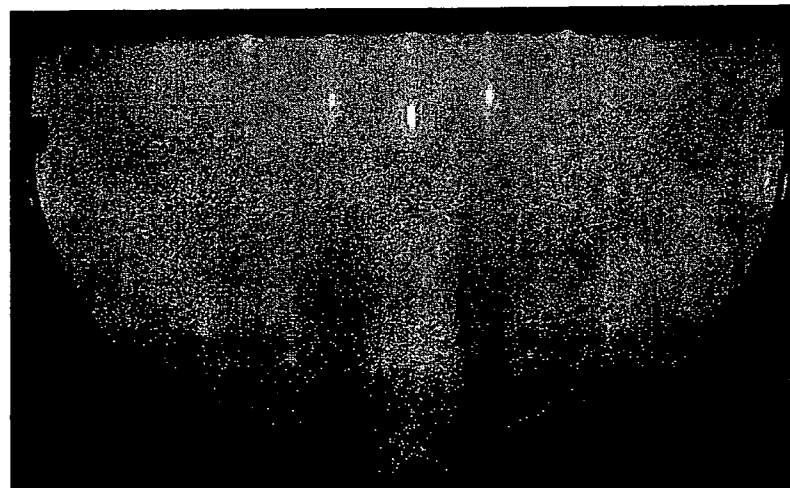


FIG. 4

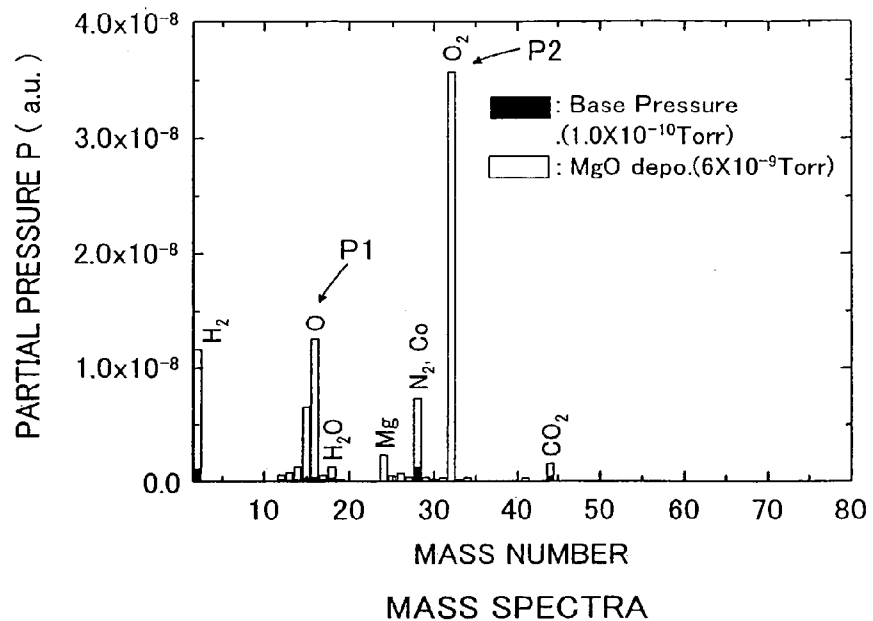


FIG. 5

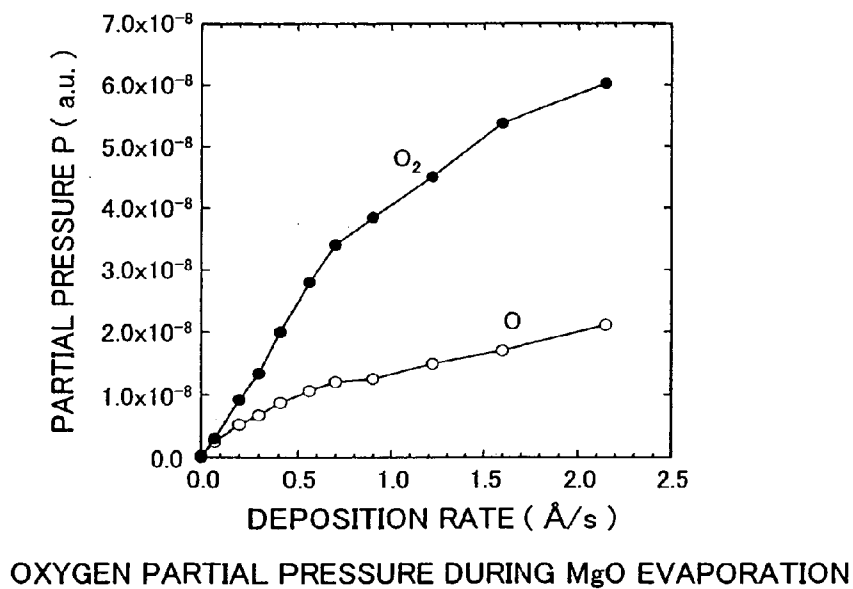




FIG. 6

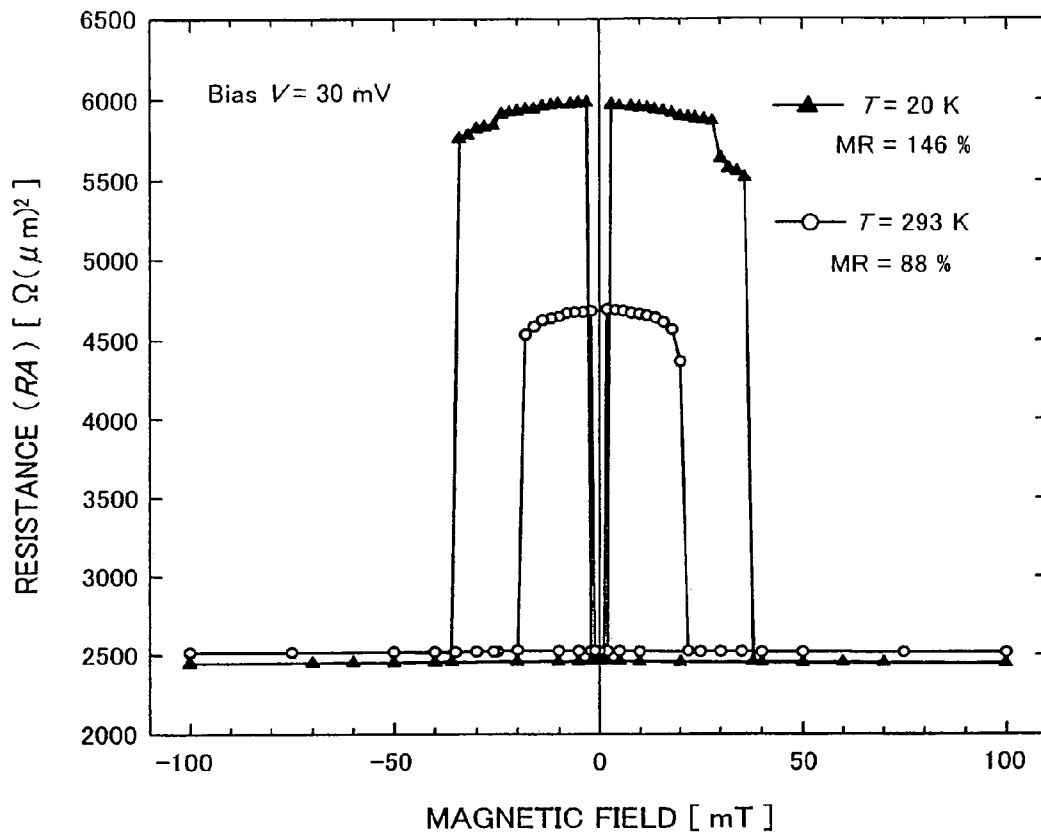


FIG. 7 (A)

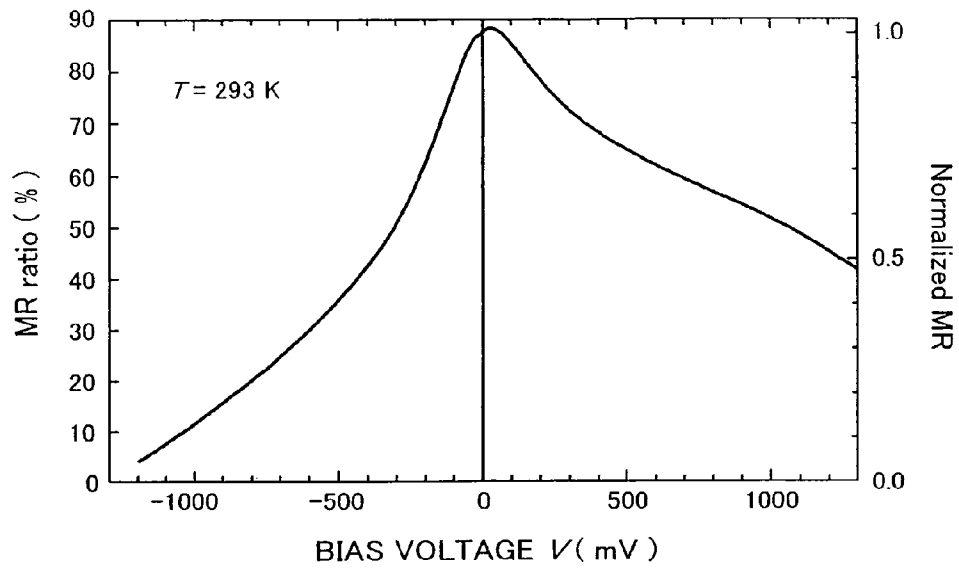


FIG. 7 (B)

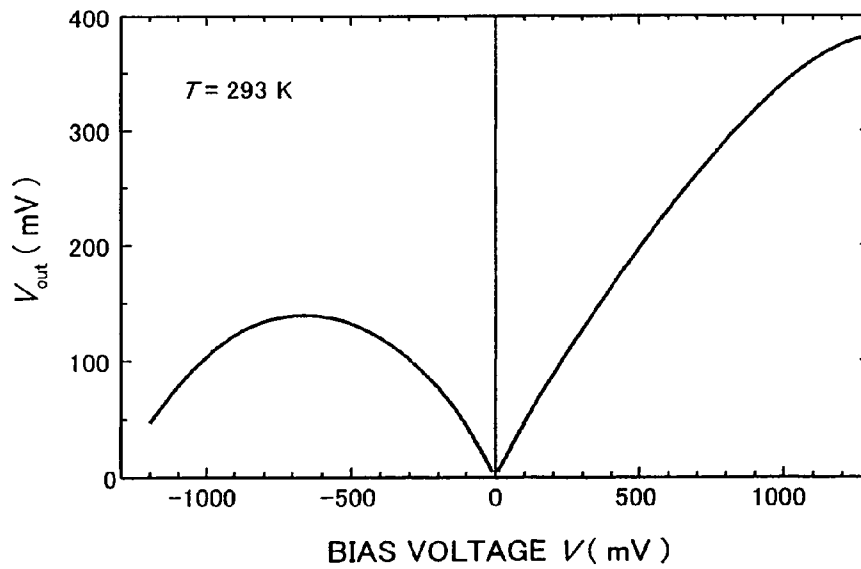


FIG. 8 (A)

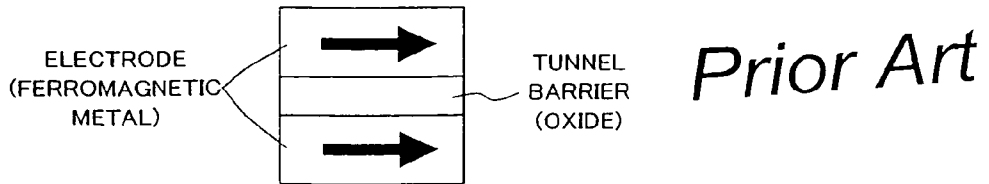


FIG. 8 (B)



FIG. 9 (A)

*Prior Art*

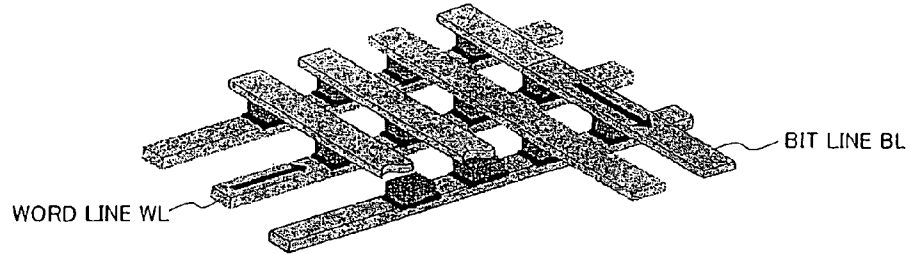


FIG. 9 (B)

*Prior Art*

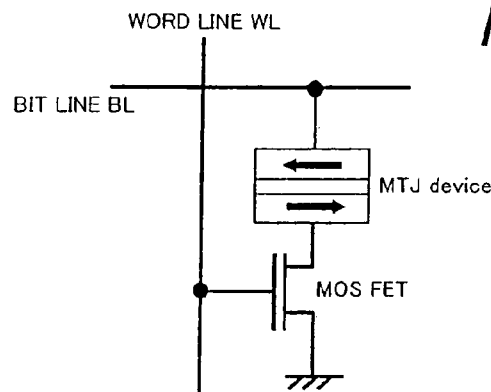


FIG. 9 (C)

*Prior Art*

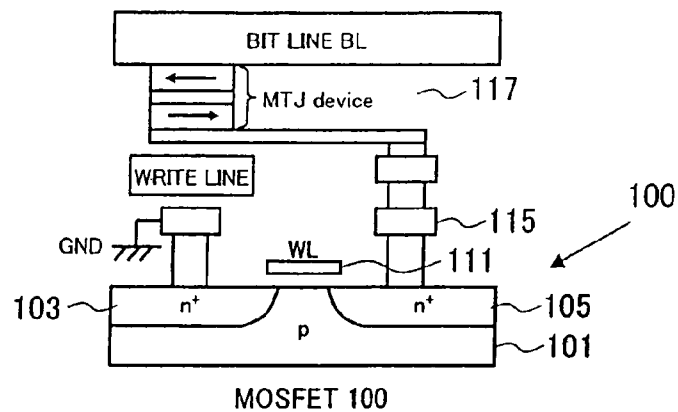


FIG. 10

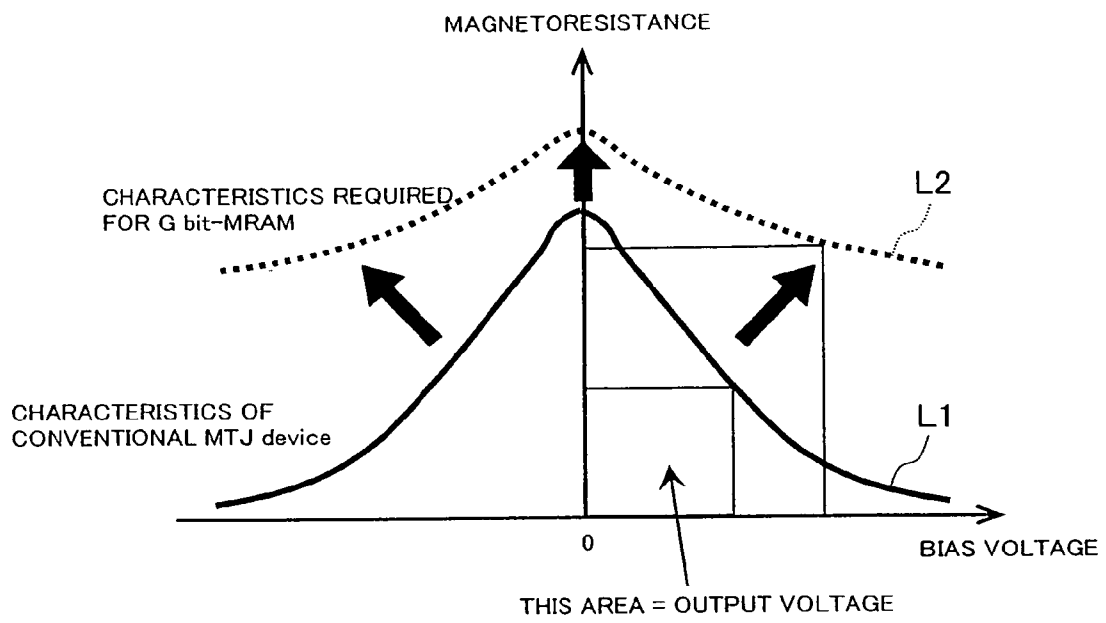
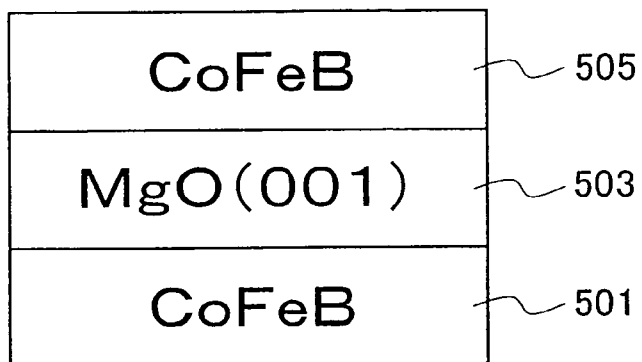


FIG. 11



## MAGNETIC TUNNEL JUNCTION DEVICE

## CROSS-REFERENCE TO RELATED APPLICATION

The present application is a Continuation of U.S. application Ser. No. 13/767,290 filed on Feb. 14, 2013, which is a Continuation of U.S. application Ser. No. 13/400,340 filed on Feb. 20, 2012, which is a Continuation of U.S. application Ser. No. 12/923,643 filed on Sep. 30, 2010, which is a Continuation of U.S. application Ser. No. 10/591,947 filed on Sep. 8, 2006, which is a National Stage Application of PCT/JP2005/004720 filed on Mar. 10, 2005. Priority is claimed from U.S. application Ser. No. 13/767,290 filed on Feb. 14, 2013, which claims priority from U.S. application Ser. No. 13/400,340 filed on Feb. 20, 2012, which claims priority from U.S. application Ser. No. 12/923,643 filed on Sep. 30, 2010, which claims priority from U.S. application Ser. No. 10/591,947 filed on Sep. 8, 2006, which claims priority from PCT/JP2005/004720 filed on Mar. 10, 2005, which claims priority from Japanese Application Nos. 2004-313350 and 2004-071186 filed Oct. 28, 2004 and Mar. 12, 2004, respectively, the content of which is hereby incorporated by reference into this application.

## BACKGROUND OF THE INVENTION

## Field of the Invention

The present invention relates to a magnetic tunnel junction device and a method of manufacturing the same, particularly to a magnetic tunnel junction device with a high magnetoresistance and a method of manufacturing the same.

## Description of Related Art

Magnetoresistive random access memories (MRAMs) refer to a large-scale integrated memory circuit that is expected to replace the currently widely used DRAM memories. Research and development of MRAM devices, which are fast and non-volatile memory devices, are being extensively carried out, and sample products of a 4 Mbit MRAM have actually been delivered.

FIGS. 8(A) and 8(B) show the structure and operation principle of a magnetic tunnel junction device (to be hereafter referred to as a "MTJ device"), which is the most important part of the MRAM. As shown in FIG. 8(A), a MTJ device comprises a tunneling junction structure in which a tunnel barrier (to be hereafter also referred to as a "barrier layer") made of an oxide is sandwiched between a first and a second electrode made of a ferromagnetic metal. The tunnel barrier layer comprises an amorphous Al—O layer (see Non-Patent Document 1). As shown in FIG. 8(A), in the case of parallel magnetization alignment where the directions of magnetizations of the first and second ferromagnetic electrodes are aligned parallel, the electric resistance of the device with respect to the direction normal to the interfaces of the tunneling junction structure decreases. On the other hand, in the case of antiparallel magnetization alignment where the directions of magnetizations of the first and second ferromagnetic electrodes are aligned antiparallel as shown in FIG. 8(B), the electric resistance with respect to the direction normal to the interfaces of the tunneling junction structure increases. The resistance value does not change in a general state, so that information "1" or "0" can be stored depending on whether the resistance value is high or not. Since the parallel and antiparallel magnetization alignments can be stored in a non-volatile fashion, the device can be used as a non-volatile memory device.

FIGS. 9(A)-9(C) show an example of the basic structure of the MRAM. FIG. 9(A) shows a perspective view of the MRAM, and FIG. 9(B) schematically shows a circuit block diagram. FIG. 9(C) is a cross-section of an example of the structure of the MRAM. Referring to FIG. 9(A), in an MRAM, a word line WL and a bit line BL are disposed in an intersecting manner, with an MRAM cell disposed at each intersection. As shown in FIG. 9(B), the MRAM cell disposed at the intersection of a word line and a bit line comprises a MTJ device and a MOSFET directly connected to the MTJ device. Stored information can be read by reading the resistance value of the MTJ device that functions as a load resistance, using the MOSFET. The stored information can be rewritten by applying a magnetic field to the MTJ device, for example. As shown in FIG. 9(C), an MRAM memory cell comprises a MOSFET 100 including a source region 105 and a drain region 103 both formed inside a p-type Si substrate 101, and a gate electrode 111 formed on a channel region that is defined between the source and drain regions. The MRAM also comprises a MTJ device 117. The source region 105 is grounded, and the drain is connected to a bit line BL via the MTJ device. A word line WL is connected to the gate electrode 111 in a region that is not shown.

Thus, a single non-volatile MRAM memory cell can be formed by a single MOSFET 100 and a single MTJ device 117. The MRAMs are therefore suitable where high levels of integration are required.

Non-Patent Document 1: D. Wang, et al.: Science 294 (2001) 1488.

## SUMMARY OF THE INVENTION

Although there are prospects for achieving MRAMs with capacities on the order of 64 Mbits based on the current technologies, the characteristics of the MTJ device, which is the heart of MRAM, needs to be improved if higher levels of integration are to be achieved. In particular, in order to increase the output voltage of the MTJ device, the magnetoresistance must be increased and the bias voltage characteristics must be improved. FIG. 10 illustrates how the magnetoresistance in a conventional MTJ device using an amorphous Al—O as the tunnel barrier changes as a function of the bias voltage (L1). As shown, in the conventional MTJ device, the magnetoresistance is small and, notably, it tends to drastically decrease upon application of bias voltage. With such characteristics, the output voltage when operation margins are taken into consideration is too small for the device to be employed for an actual memory device. Specifically, the magnetoresistance of the current MTJ device is small at approximately 70%, and the output voltage is also small at no more than 200 mV, which is substantially half the output voltage of a DRAM. This has resulted in the problem that as the level of integration increases, signals are increasingly lost in noise and cannot be read.

It is an object of the invention to increase the output voltage of a MTJ device. It is another object of the invention to provide a memory device with a high magnetoresistance for stable operation.

In one aspect, the invention provides a magnetoresistive device comprising a magnetic tunnel junction structure comprising: a tunnel barrier layer; a first ferromagnetic material layer of the BCC structure formed on a first side of the tunnel barrier layer; and a second ferromagnetic material layer of the BCC structure formed on a second side of the tunnel barrier layer, wherein the tunnel barrier layer is formed by a single-crystal MgO<sub>x</sub> (001) layer or a poly-

crystalline  $\text{MgO}_x$  ( $0 < x < 1$ ) layer in which the (001) crystal plane is preferentially oriented.

The invention further provides a magnetoresistive device comprising a magnetic tunnel junction structure comprising: a tunnel barrier layer comprising  $\text{MgO}(001)$ ; a first ferromagnetic material layer comprising  $\text{Fe}(001)$  formed on a first side of the tunnel barrier layer; and a second ferromagnetic material layer comprising  $\text{Fe}(001)$  formed on a second side of the tunnel barrier layer, wherein the  $\text{MgO}$  layer is formed by a single-crystalline  $\text{MgO}_x$  (001) layer or a polycrystalline  $\text{MgO}_x$  ( $0 < x < 1$ ) layer in which the (001) crystal plane is preferentially oriented. In a preferred embodiment, the band discontinuity value (the height of the tunnel barrier) between the bottom of the conduction band of the  $\text{MgO}(001)$  layer and the Fermi energy of the  $\text{Fe}(001)$  layer is smaller than an ideal value of a perfect single-crystal without defect. These features increase the magnetoresistance and thereby allow the output voltage of the MTJ device to be increased. By using any of the aforementioned MTJ devices as a load for a single transistor, a non-volatile memory can be formed.

In another aspect, the invention provides a method of manufacturing a magnetoresistive device comprising: preparing a substrate; depositing a first  $\text{Fe}(001)$  layer on the substrate; depositing a tunnel barrier layer on the first  $\text{Fe}(001)$  layer by electron beam evaporation under high vacuum, the tunnel barrier layer comprising a single-crystalline  $\text{MgO}_x$  (001) or a poly-crystalline  $\text{MgO}_x$  ( $0 < x < 1$ ) in which the (001) crystal plane is preferentially oriented; and forming a second  $\text{Fe}(001)$  layer on the tunnel barrier layer.

The invention furthermore provides a method of manufacturing a MTJ device comprising a first step of preparing a substrate comprising a single-crystalline  $\text{MgO}_x$ (001) or a poly-crystalline  $\text{MgO}_x$  ( $0 < x < 1$ ) in which the (001) crystal plane is preferentially oriented, a second step of depositing a first  $\text{Fe}(001)$  layer on the substrate and performing an annealing process to make the surface flat, a third step of depositing a tunnel barrier layer on the first  $\text{Fe}(001)$  layer by electron beam evaporation, the tunnel barrier layer comprising a single-crystalline  $\text{MgO}_x$ (001) or a poly-crystalline  $\text{MgO}_x$  ( $0 < x < 1$ ) in which the (001) crystal plane is preferentially oriented, and a fourth step of forming a second  $\text{Fe}(001)$  layer on the tunnel barrier layer. The method may further comprise the step of growing a seed layer between the first and the second steps, the seed layer comprising a single-crystalline  $\text{MgO}_x$ (001) or a poly-crystalline  $\text{MgO}_x$  ( $0 < x < 1$ ) in which the (001) crystal plane is preferentially oriented. The  $\text{MgO}$  layer may be deposited using a target with the value of  $x$  in  $\text{MgO}_x$  adjusted. The value of  $x$  in  $\text{MgO}_x$  may be adjusted in the step of forming the  $\text{MgO}$ .

In yet another aspect, the invention provides a magnetoresistive device comprising a magnetic tunnel junction structure comprising a tunnel barrier layer comprising  $\text{MgO}(001)$ , a first ferromagnetic material layer comprising an amorphous magnetic alloy formed on a first side of the tunnel barrier layer, and a second ferromagnetic material layer comprising an amorphous magnetic alloy formed on a second side of the tunnel barrier layer, wherein the discontinuous value (the height of the tunnel barrier) between the bottom of the conduction band of the  $\text{MgO}(001)$  layer and the Fermi energy of the first or the second ferromagnetic material layer comprising the amorphous magnetic alloy is lower than an ideal value of a perfect single-crystal with no defect.

#### BRIEF DESCRIPTION OF THE DRAWINGS

FIG. 1(B) shows the structure of a MTJ device according to a first embodiment of the invention, and FIG. 1(A) shows

the energy band structure of a ferromagnetic metal  $\text{Fe}(001)$ , illustrating the  $E-E_F$  relationship with respect to the [001] direction of the momentum space.

FIG. 2(A) to FIG. 2(D) schematically show the process of manufacturing a MTJ device with a  $\text{Fe}(001)/\text{MgO}(001)/\text{Fe}(001)$  structure (to be hereafter referred to as a “ $\text{Fe}(001)/\text{MgO}(001)/\text{Fe}(001)$  MTJ device”) according to an embodiment of the invention.

FIG. 3(A) shows a RHEED image of a  $\text{Fe}(001)$  lower electrode (a first electrode), and FIG. 3(B) shows a RHEED image of a  $\text{MgO}(001)$  barrier layer.

FIG. 4 shows the results of observing the quadrupole mass spectra in the deposition chamber during the  $\text{MgO}$  evaporation.

FIG. 5 shows the film deposition rate dependency of the oxygen partial pressure during the  $\text{MgO}$  evaporation.

FIG. 6 shows typical magnetoresistance curves of the  $\text{Fe}(001)/\text{MgO}(001)/\text{Fe}(001)$  MTJ device.

FIG. 7(A) shows the bias voltage dependency of the MR ratio at room temperature, and FIG. 7(B) shows the output voltage  $V_{out}$  of the MTJ device (=bias voltage $\times$ ( $R_{ap}-R_p$ )/ $R_p$ ).

FIGS. 8(A) and 8(B) show the structure of the MTJ device and its operating principle.

FIGS. 9(A)-9(C) show an example of the basic structure of an MRAM, FIG. 9(A) showing a perspective view of the MRAM, FIG. 9(B) showing a schematic circuit diagram, and FIG. 9(C) showing a cross-sectional view of an example of its structure.

FIG. 10 shows how the magnetoresistance of a conventional MTJ device using an amorphous  $\text{Al}-\text{O}$  as the tunnel barrier changes depending on the bias voltage.

FIG. 11 shows the structure of a MTJ device according to a variation of the invention, corresponding to FIG. 1(B).

#### DESCRIPTION OF THE PREFERRED EMBODIMENTS

In the context of the present specification, because  $\text{MgO}$  has a cubic crystal structure (NaCl structure), the (001) plane, the (100) plane, and the (010) plane are all equivalent. The direction perpendicular to the film surface is herein considered to be the  $z$ -axis so that the film plane can be uniformly described as (001). Also in the context of the present specification, BCC structure, which the crystalline structure of ferromagnetic electrode layer, means body-centered cubic lattice structure. More specifically, BCC structure includes the BCC structure with no chemical ordering so-called A2-type structure, the BCC structure with chemical ordering such as B2-type structure and  $L2_1$ -type structure, and also the aforementioned structures with slight lattice distortion.

The term “ideal value” with regard to a perfect single-crystal without defect herein refers to a value that has been estimated from ultraviolet photoemission spectroscopy experiments (see W. Wulfhekel, et al.: Appl. Phys. Lett. 78 (2001) 509.). The term “ideal value” is used herein because the aforementioned state can be considered to be an upper limit value of the potential barrier height of the tunnel barrier of an ideal single-crystal  $\text{MgO}$  with hardly any oxygen vacancy defect or lattice defect.

Before describing the preferred embodiments of the invention, an analysis conducted by the inventors is discussed. The magnetoresistance (MR) ratio of a MTJ device can be expressed by the following equation:

$$\Delta R/R_p = (R_{ap} - R_p)/R_p$$



where  $R_p$  and  $R_{ap}$  indicate the tunnel junction resistance in the cases of parallel and antiparallel magnetization alignments, respectively, of two electrodes. According to the Jullire's formula, the MR ratio at low bias voltage can be expressed by:

$$MR \text{ ratio} = (R_{ap} - R_p) / R_p = 2P_1 P_2 / (1 - P_1 P_2), \text{ and}$$

$$P\alpha = (D\alpha\uparrow(E_F) - D\alpha\downarrow(E_F)) / (D\alpha\uparrow(E_F) + D\alpha\downarrow(E_F)),$$

$$\text{where } \alpha = 1, 2 \quad (1)$$

In the above equations,  $P\alpha$  is the spin polarization of an electrode, and  $D\alpha\uparrow(E_F)$  and  $D\alpha\downarrow(E_F)$  are the density of state (DOS) at the Fermi energy ( $E_F$ ) of the majority-spin band and the minority-spin band, respectively. Since the spin polarization of ferromagnetic transition metals and alloys is approximately 0.5 or smaller, the Jullire's formula predicts a highest estimated MR ratio of about 70%.

Although the MR ratio of approximately 70% has been obtained at room temperature when a MTJ device was made using an amorphous Al—O tunnel barrier and polycrystalline electrodes, it has been difficult to obtain the output voltage of 200 mV, which is comparable to the output voltages of DRAMs, thereby preventing the realization of MRAM as mentioned above.

The inventors tried an approach to deposit a MTJ device in which the tunnel barrier comprises a single-crystal (001) of magnesium oxide (MgO) or a poly-crystalline MgO in which the (001) crystal plane is preferentially oriented. It is the inventors' theory that, because magnesium oxide is a crystal (where the atoms are arranged in an orderly fashion), as opposed to the conventional amorphous Al—O barrier, the electrons are not scattered and the coherent states of electrons are conserved during the tunneling process. FIG. 1(B) shows the MTJ device structure according to an embodiment of the invention. FIG. 1(A) shows the energy band structure of the ferromagnetic Fe(001), that is, the  $E-E_F$  relationship with respect to the [001] direction of the momentum space. As shown in FIG. 1(B), the MTJ device structure of the present embodiment comprises a first Fe (001) layer **1**, a second Fe (001) layer **5**, and a single-crystalline  $MgO_x$  (001) layer **3** or a poly-crystalline  $MgO_x$  ( $0 < x < 1$ ) layer **3** sandwiched therebetween, the polycrystalline layer having the (001) crystal plane preferentially oriented therein. According to the aforementioned Jullire's model, assuming that the momentum of the conduction electrons is preserved in the tunneling process, the tunneling current that passes through MgO would be dominated by those electrons with wave vector  $k_z$  in the direction perpendicular to the tunnel barrier (normal to the junction interfaces). In accordance with the energy band diagram shown in FIG. 1(A) of Fe in the [001] ( $\Gamma$ -H) direction, the density of state (DOS) at the Fermi energy  $E_F$  does not exhibit a very high spin polarization due to the fact that the sub-bands of the majority-spin and the minority-spin have states at the Fermi energy  $E_F$ . However, in case the coherent states of electrons are conserved in the tunneling process, only those conduction electrons that have totally symmetrical wave functions with respect to the axis perpendicular to the barrier would be coupled with the states in the barrier region and come to have a finite tunneling probability. The  $\Delta_1$  band in the Fe(001) electrode has such totally symmetric wave functions. As shown in FIG. 1(A), the majority spin  $\Delta_1$  band (solid line) has states at the Fermi energy  $E_F$ , whereas the minority spin  $\Delta_1$  band (broken line) does not have state at the Fermi energy  $E_F$ . Because of such half-metallic characteristics of the Fe  $\Delta_1$  band, there is the possibility that a very

high MR ratio can be obtained in a coherent spin polarized tunneling. Since in an epitaxial (single-crystal, or (001) oriented poly-crystal) MTJ device the scattering of electrons is suppressed during the tunneling process, an epitaxial MTJ device is thought to be ideal for realizing the aforementioned coherent tunneling.

In the following, a MTJ device according to a first embodiment of the invention and a method of manufacturing the same will be described with reference to the drawings.

FIGS. 2(A) to 2(D) schematically show the method of manufacturing the MTJ device having the Fe (001)/MgO (001)/Fe(001) structure according to the embodiment (to be hereafter referred to as a "Fe(001)/MgO(001)/Fe(001) MTJ device"). Fe(001) refers to a ferromagnetic material with the BCC structure. First, a single-crystal MgO(001) substrate **11** was prepared. In order to improve the morphology of the surface of the single-crystal MgO(001) substrate **11**, a MgO (001) seed layer **15** was grown by the molecular beam epitaxy (MBE) method. This was subsequently followed by the growth of an epitaxial Fe(001) lower electrode (first electrode) **17** with the thickness of 50 nm on the MgO(001) seed layer **15** at room temperature, as shown in FIG. 1(B), and then annealing was performed at 350° C. under ultrahigh vacuum ( $2 \times 10^{-8}$  Pa). Electron-beam evaporation conditions included an acceleration voltage of 8 kV, a growth rate of 0.02 nm/sec, and the growth temperature of room temperature (about 293K). The source material of the electron-beam evaporation was MgO of the stoichiometric composition (the ratio of Mg to O being 1:1), the distance between the source and the substrate was 40 cm, the base vacuum pressure was  $1 \times 10^{-8}$  Pa, and the  $O_2$  partial pressure was  $1 \times 10^{-6}$  Pa. Alternatively, a source with oxygen vacancy defects may be used instead of the MgO of the stoichiometric composition (the ratio of Mg to O is 1:1).

FIG. 3(A) shows a RHEED image of the Fe(001) lower electrode (a first electrode). The image shows that the Fe(001) lower electrode (first electrode) **17** possesses a good crystallinity and flatness. Thereafter, a MgO(001) barrier layer **21** with the thickness of 2 nm was epitaxially grown on the Fe(001) lower electrode (first electrode) at room temperature, also using the MgO electron-beam evaporation method. FIG. 3(B) shows a RHEED image of the MgO(001) barrier layer **21**. The image shows that the MgO(001) barrier layer **21** also possesses a good crystallinity and flatness.

As shown in FIG. 2(D), a Fe(001) upper electrode (a second electrode) **23** with the thickness of 10 nm was formed on the MgO(001) barrier layer **21** at room temperature. This was successively followed by the deposition of a Co layer **25** with the thickness of 10 nm on the Fe(001) upper electrode (second electrode) **23**. The Co layer **25** is provided to increase the coercive force of the upper electrode **23** so as to realize the antiparallel magnetization alignment. The thus prepared sample was then processed by microfabrication techniques to obtain the Fe(001)/MgO (001)/Fe(001) MTJ device.

The aforementioned MgO evaporation using an electron beam involved the formation of a film under ultrahigh vacuum of  $10^{-9}$  Torr. It can be seen that in this method, the film, even when formed on a glass substrate to the thickness of 300 nm, was colorless and transparent, showing that a good crystal film was formed. FIG. 4 shows the results of observing the quadrupole mass spectra in the deposition chamber during the MgO growth. The results show that the partial pressures regarding the spectrum P1 of O and the spectrum P2 of  $O_2$  are high. FIG. 5 shows the film deposition rate dependency of the oxygen partial pressure during MgO evaporation. It will be seen from the figure that the oxygen

partial pressure itself is high, and that the oxygen partial pressure increases as the deposition rate increases. These results indicate the separation of oxygen from MgO during the deposition of MgO. Since the separated oxygen is pumped out of the deposition chamber using vacuum pumps, there is the possibility that there are oxygen vacancy defects such as  $MgO_x$  ( $0.9 < x < 1$ ). When there are oxygen vacancy defects, the potential barrier height of the MgO tunnel barrier is thought to decrease (such as in the range of 0.10 to 0.85 eV; more specifically, 0.2 to 0.5 eV), which is thought to result in an increase in the tunneling current. In the case of a typical Al-O tunnel barrier, the height of the tunnel barrier with respect to Fe(001) electrodes is considered to be 0.7 to 2.5 eV. An ideal tunnel barrier height of a MgO crystal is 3.6 eV, and experimental values of 0.9 to 3.7 eV have been obtained. Using the method according to the present embodiment of the invention, a tunnel barrier height of approximately 0.3 eV is expected, indicating that the resistance of the tunnel barrier can be lowered. However, it should be noted that other factors, such as the influence of the aforementioned coherent tunneling, might also be involved. The value of  $x$  in  $MgO_x$  due to oxygen vacancy defects is such that  $0.98 < x < 1$ , and more preferably  $0.99 < x < 1$ . These are the ranges such that the sole presence of Mg is excluded and the characteristics of MgO can be basically maintained.

The aforementioned tunnel barrier height  $\phi$  was determined by fitting the electric conductance characteristics of the MTJ device (the relationship between tunnel current density  $J$  and bias voltage  $V$ ) onto the Simmons' formula (Equation (20) in a non-patent document by J. G. Simmons: J. Appl. Phys. 34, pp. 1793-1803 (1963)) based on the WKB approximation, using the least squares method. The fitting was performed using the free electron mass ( $m=9.11 \times 10^{-31}$  kg) as the electron's effective mass. When a bias voltage  $V$  (which is normally on the order of 500 mV to 1000 mV) is applied until non-linearity appears in the J-V characteristics, the height  $\phi$  of the tunnel barrier and the effective thickness  $\Delta s$  of the tunnel barrier can be simultaneously determined by fitting the J-V characteristics using the Simmons' formula.

The effective thickness  $\Delta s$  of the tunnel barrier was determined to be smaller than the thickness of the actual MgO(001) tunnel barrier layer ( $t_{MgO}$ ) determined from a cross-sectional transmission electron microscope image of the MTJ device by approximately 0.5 nm. This is the result of the effective thickness  $\Delta s$  of the tunnel barrier having been reduced from the actual MgO(001) layer thickness by the effect of the image potential produced at the interface between the MgO(001) layer and the alloy layer consisting mainly of Fe and Co.

It is noted that, in the event that  $t_{MgO}$  can be accurately determined using the cross-sectional transmission electron microscope (TEM) image, the height  $\phi$  of the tunnel barrier can be more simply determined by the following technique. Namely, when the bias voltage  $V$  applied to the MTJ device is small (normally 100 mV or smaller), the tunnel current density  $J$  is proportional to the bias voltage  $V$ , such that the J-V characteristics become linear. In such a low-bias voltage region, the Simmons' formula can be described as follows:

$$J = [2m\phi]^{1/2} / \Delta s (e/h)^2 \exp[-(4\pi\Delta s/h) \times (2m\phi)^{1/2}] \times V \quad (2)$$

where  $m$  is the mass of the free electron ( $9.11 \times 10^{-31}$  kg),  $e$  is the elementary electric charge ( $1.60 \times 10^{-19}$  C), and  $h$  is the Planck's constant ( $6.63 \times 10^{-34}$  J·s). The effective thickness of the tunnel barrier  $\Delta s$  is approximately  $t_{MgO} - 0.5$  nm. By fitting the J-V characteristics of the MTJ device in the

low-bias voltage region onto Equation (2), the height  $\phi$  of the tunnel barrier can be simply and yet accurately estimated.

FIG. 6 shows a typical magnetoresistance curve of the Fe(001)/MgO(001)/Fe(001) MTJ device produced by the above-described method. The MR ratio is 146% at the measurement temperature of 20K and 88% at the measurement temperature of 293K. These values represent the highest MR ratios that have so far been obtained at room temperature. Such high MR ratios cannot be explained by the spin polarization of the Fe(001) electrode and is thought rather to be related to a coherent spin-polarized tunneling. When 160 prototype MTJ devices were made, the variations regarding the MR ratio and tunneling resistance value were not more than 20%. The yield of the MTJ devices was 90% or more at the laboratory stage. These high values suggest the effectiveness of the approach of the invention. The resistance-area (RA) product of the MTJ device was on the order of a few  $k\Omega\mu m^2$ , which is suitable for MRAM.

FIG. 7(a) shows the bias voltage dependency of the MR ratio at room temperature. It will be seen that the bias voltage dependency of the MR ratio is fairly small. Although the characteristics are asymmetric, the voltage  $V_{half}$  at which the MR ratio is reduced in half of the zero-bias value is 1250 mV, which is a very high value. In this connection, it is noted that the voltage  $V_{half}$  at which the MR ratio is reduced in half of the zero-bias value in the conventional MTJs with Al—O tunnel barrier is 300 to 600 mV. FIG. 7(b) shows the output voltage  $V_{out}$  of the MTJ device (=bias voltage  $\times$  (Rap—Rp)/Rap). The maximum value of the output voltage  $V_{out}$  is 380 mV with a positive bias. This value is about twice as large as that (a little less than 200 mV) in the case of the Al—O barrier. These high values in terms of both MR ratio and output voltage suggest the effectiveness of the technique according to the present embodiment.

Although in the above-described embodiment Fe(001) of BCC was employed, an Fe alloy of BCC, such as an Fe—Co alloy, Fe—Ni alloy, or Fe—Pt alloy, may be used instead. Alternatively, a layer of Co or Ni with the thickness of one or several monoatomic layers may be inserted between the electrode layer and the MgO(001) layer.

Hereafter, a MTJ device according to a second embodiment of the invention and a method of manufacturing the same will be described. In the method of manufacturing a Fe(001)/MgO(001)/Fe(001) MTJ device according to the present embodiment, MgO(001) is initially deposited in a poly-crystalline or amorphous state by sputtering or the like, and then an annealing process is performed such that a poly-crystal in which the (001) crystal plane is preferentially oriented or a single-crystal is obtained. The sputtering conditions were such that, for example, the temperature was room temperature (293K), a 2-inch  $\phi$  MgO was used as a target, and sputtering was conducted in an Ar atmosphere. The acceleration power was 200 W and the growth rate was 0.008 nm/s. Because MgO that is deposited under these conditions is in an amorphous state, a crystallized MgO was obtained by increasing the temperature to 300° C. from room temperature and maintaining that temperature for a certain duration of time.

Oxygen vacancy defects may be introduced by a method whereby oxygen vacancy defects is produced during growth, a method whereby oxygen vacancy defects is introduced subsequently, or a method whereby a state with oxygen vacancy defects is subjected to an oxygen plasma process or natural oxidation so as to achieve a certain oxygen deficit level.

As described above, in accordance with the MTJ device technology of the present embodiment, an annealing process is carried out for crystallization after an amorphous MgO has been deposited by sputtering, thereby eliminating the need for large-sized equipment.

Hereafter, a MTJ device according to a variation of the embodiments of the invention will be described with reference to the drawings. FIG. 11 shows the structure of the MTJ device according to the variation, which corresponds to FIG. 1(B). As shown in FIG. 11, the MTJ device of the variation is characterized in that, as in the MTJ device of the above-described embodiments, the electrodes disposed on either side of a single-crystal MgO<sub>x</sub>(001) layer 503 or an oxygen-deficit poly-crystal MgO<sub>x</sub> (0<x<1) in which the (001) crystal plane is preferentially oriented comprises an amorphous ferromagnetic alloy, such as CoFeB layers 501 and 505. The amorphous ferromagnetic alloy can be formed by evaporation or sputtering, for example. The resultant characteristics are substantially identical to those of the first embodiment.

As the amorphous magnetic alloy, FeCoB, FeCoBSi, FeCoBP, FeZr, and CoZr may be used, for example. Although an anneal process after the preparation of the MTJ device might cause the amorphous magnetic alloy in the electrode layers to be partially or entirely crystallized, this would not lead to a significant deterioration of the MR ratio. Thus, such a crystallized amorphous magnetic alloy may be used in the electrode layers.

While the MTJ device according to various embodiments of the invention has been described, it should be apparent to those skilled in the art that the invention is not limited to those specific embodiments and various other modifications, improvements and combinations are possible. For example, the height of the tunnel barrier may be adjusted by doping Ca or Sr, instead of introducing an oxygen vacancy defects to the MgO layer. Further, while the MgO layer has been described to be deposited by electron-beam evaporation or sputtering, it should be obvious that other deposition methods are also possible. The term “high vacuum” refers to values on the order of no more than 10<sup>-6</sup> Pa in the case where oxygen is not introduced, for example. In the case where oxygen is introduced, the term refers to values on the order of 10<sup>-4</sup> Pa.

In accordance with the invention, a larger magnetoresistance than in the conventional MTJ device can be obtained, and the output voltage of the MTJ device can be increased. At the same time, the resistance value of the MTJ device can be reduced so that it is optimized for MRAM. The invention thus enables the level of integration of MRAM using the MTJ device to be readily increased. In accordance with the

invention, the output voltage value of the MRAM roughly doubles over prior art, making the MTJ device of the invention suitable for very large scale integrated MRAMs of gigabit class.

What is claimed is:

1. A tunnel barrier layer disposed between a first ferromagnetic material layer and a second ferromagnetic material layer that are disposed over a substrate, wherein the tunnel barrier layer comprises a poly-crystalline magnesium oxide layer in which a (001) crystal plane is preferentially oriented, wherein the first ferromagnetic material layer is composed of an Fe—Co alloy of BCC which alloy comprises Fe, Co, and B, wherein the first ferromagnetic material layer is located between the tunnel barrier layer and the substrate.
2. The tunnel barrier layer according to claim 1, wherein a barrier height of the tunnel barrier layer is in a range of 0.2 to 0.5 eV.
3. The tunnel barrier layer according to claim 2, wherein the barrier height p of the tunnel barrier layer is obtained by fitting J-V characteristics of a tunnel barrier junction structure to an equation (1):

$$J=[(2m\phi)^{1/2}/\Delta s](e/h)^2 \times \exp[-(4\pi\Delta s/h) \times (2m\phi)^{1/2}] \times V \quad (1)$$

where J is a tunnel current density flowing through the tunnel barrier layer, V is an applied bias voltage that is 100 mV or smaller, m is the free electron mass, e is the elementary electric charge, h is the Planck’s constant, Δs is an effective thickness of the tunnel barrier layer that is approximately equivalent to (t<sub>MgO</sub>-0.5 nm), and t<sub>MgO</sub> is an actual thickness of the tunnel barrier layer determined using a cross-sectional transmission electron microscope image.

4. The tunnel barrier layer according to claim 1, wherein the second ferromagnetic material layer is composed of an alloy comprising Fe and Co, and wherein the second ferromagnetic material layer is located above the tunnel barrier layer.
5. The tunnel barrier layer according to claim 1, wherein the second ferromagnetic material layer is composed of an alloy comprising Fe, Co, and B, and wherein the second ferromagnetic material layer is located above the tunnel barrier layer.
6. The tunnel barrier layer according to claim 1, wherein the tunnel barrier layer is disposed on the first ferromagnetic material layer.

\* \* \* \* \*